J. Appl Phys (in press) Presented at MMM Conference, Minneapolis, MN, Nov. '93

(2)

BC-01
10/5/93

Tribological Studies of Silicon for Magnetic Recording Applications (Invited)

Bharat Bhushan and Vilas N. Koinkar

Computer Microtribology and Contamination Laboratory

Department of Mechanical Engineering

The Ohio State University, Columbus, Ohio 43210-1107

Abstract

Read-write sliders made of silicon using integrated-circuit technology offer advantages of low-cost and high volume production. In the present study our objective is to investigate whether the friction and wear performance of bare silicon is adequate for disk drive application or whether certain coatings/treatments are necessary for low friction and wear. Macrotribological experiments have been performed with various pin/slider materials and magnetic disks in a modified disk drive. Microtribological studies have also been conducted on silicon using a friction force microscope. Based on macrotests, we found that the friction and wear performance of bare silicon is not adequate. With single and polycrystalline silicon, transfer of amorphous carbon from the disk to the pin/slider and oxidation-enhanced fracture of pin/slider material followed by oxidation of the transfer coating is responsible for degradation of the sliding interface and consequent friction increase in ambient air. With dry-oxidized or PECVD-SiO_2-coated silicon, no significant friction increase or interfacial degradation was observed in ambient air. In the absence of an oxidizing environment (in dry nitrogen), the coefficient of friction decreased from 0.2 to 0.05 following amorphous carbon transfer for the materials tested. Nanoscratching/nanowear and nanoindentation studies also indicate that coated silicon is superior to bare silicon. Macro-and micro-coefficient of friction values of all samples are found to be about the same with the microvalues lower than the macrovalues. Based on this study, we conclude that coated silicon is an excellent candidate for the construction of magnetic head sliders.

PACS numbers: 61.16 P, 61.80, 68.20, 81.60

I. INTRODUCTION

The advantages of miniaturization and low-cost are resulting in an increasing use of silicon as a mechanical material[1,2]. Read-write sliders made of silicon have been fabricated using integrated circuit technology[3,4]. Integrated circuit technology offers the advantages of low cost and high volume production. However, limited data exist on the tribological behavior of silicon as to be used in the disk drives[4-9]. In the present study our objective is to evaluate the friction and wear performance of silicon with and without coatings and surface treatments, in sliding contact with lubricated and unlubricated amorphous carbon coated thin-film disks for potential use as a slider material[10]. Results from experiments performed with commonly used slider materials (Al_2O_3-TiC and Mn-Zn Ferrite) are also presented for comparison.

To further understand the tribological properties of silicon material, microtribological tests were conducted on the bare and treated silicon. Nanoscratching/wear, nanoindentation and microfriction measurements have been made using a friction force microscope[11-13]. Results of macro and microtribological studies are the subject of this paper.

II. EXPERIMENTAL

A. Macrotribological measurement techniques

Experiments have been performed with various pin/slider materials and magnetic disks in a modified disk drive capable of rotating the magnetic disks at variable speeds from 100 to 3600 rpm. The pin or slider to be tested was glued onto a suspension and mounted on a crossed I-beam fixture which was instrumented with semiconductor strain gauges to measure the normal and frictional forces exerted on the pin or slider. The output of the strain gauge was fed to a PC via a A/D converter. The entire setup was housed inside a bell jar assembly which could be evacuated to 0.13 Pa (10^{-3} Torr) and backfilled or purged with a gas to allow experiments to be conducted in desired environments[10]. The normal load used in the experiments was 0.15 N and the sliding speeds at track radii ranging from 45-55 mm varied from 0.9-1.2 m/s. At these speeds the pin remained in contact throughout the period of testing to simulate start/stop conditions.

B. Microtribological measurement techniques

Microtribological experiments have been performed using a friction force microscope (FFM), to conduct studies of scratching, wear, indentation and friction[11,13]. Simultaneous measurements of friction force and surface roughness can be made using this instrument. A single-crystal natural diamond tip was used for nanoscratch, nanowear and nanoindentation measurements at relatively higher loads (10 μN to 150 μN). The tip was ground to the shape of a three-sided pyramid with an apex angle of 80° whose point was sharpened to a radius of about 100 nm. The tip was mounted on a stainless steel beam with a normal stiffness of about 25 N/m[12,13]. A microfabricated Si_3N_4 tip on a beam with a stiffness of 0.4 N/m (at a normal load 10-150 nN) was used for topographic imaging and friction force measurements. The tip was square pyramidal with a tip radius of about 30 nm.

For scratching and wear, the sample was scanned in a direction orthogonal to the long axis of the cantilever beam at a scanning speed of 1 μm/s. For wear, an area of 2 μm x 2 μm was scanned. Sample surfaces were scanned before and after the scratch or wear to obtain the initial and the final surface topography at a load of about 0.5 μN, over an area larger than the scratched or worn region to observe the scratch or wear scars. The operation procedures for nanoindentation were similar to those used for nanowear except that the scan size was set to zero in the case of nanoindentation, in order for the tip to continuously press the sample surface for about two seconds. The surface was imaged before and after the indentation at a normal load of about 0.5 μN. Nanohardness was calculated by dividing the indentation load by the projected residual area. For measurement of friction force, the sample was scanned over 500 nm x 500 nm area in a direction orthogonal to the long axis of the cantilever beam with a scan rate of 5 Hz (scanning speed of 2.5 μm/s).

C. Test samples

The disks used in the macro experiments were commercially available 130-mm diameter thin-film rigid disks. The lubricated disk structure consisted of a circumferentially-textured 1.3-mm thick Al-Mg alloy substrate with a 10-20 μm thick electroless plated Ni-P coating, about 75-nm thick ($Co_{79}Pt_{14}Ni_7$) magnetic coating, 20-30 nm thick diamondlike carbon (DLC) coating, and 0.5-2 nm thick Z-Dol perfluoropolyether lubricant coating[10]. The unlubricated disks did not contain the lubricant coating. The surface roughness of the disks used was about 7-8 nm rms and about 40 nm peak to valley distance

as measured using an optical profiler[10]. The pins and wafers used in the macro experiments were made of single and polycrystalline silicon, Mn-Zn ferrite and Al_2O_3-TiC. Single-crystal silicon of (111), (110) and (100) orientations were tested. The grain size of the polycrystalline silicon samples was about 5 mm. The pins were 3.5 mm square and 850 μm thick and were lapped to provide a large radius of curvature of 100 μm to the contacting surface to avoid edge effects during testing. The pins were lapped to a surface roughness of less than 1 nm rms as measured by optical profiler. Commercial full size sliders (rail dimensions: 3.6 mm x 0.4 mm) were also used in the experiments[10]. The maximum normal Hertzian contact stresses for a silicon pin and slider at a normal load of 0.15 N were about 40 MPa and 5 kPa respectively. Besides virgin silicon pins, thermally oxidized (under both wet and dry conditions), plasma enhanced chemical vapor deposition (PECVD) oxide coated and ion implanted single-crystal silicon pins of orientation (111) were also tested. Thermal oxidation of silicon pins was carried out in a quartz furnace at temperatures of 900-1000°C in dry oxygen and moisture-containing oxygen ambients. The latter condition was achieved by passing dry oxygen through boiling water before entering the furnace. The thickness of the thermal oxide on the silicon pins used in the present investigation was about 0.5 μm for dry oxidation and about 1 μm for wet oxidation. The oxide thicknesses were measured by using stylus profiler (alpha-step 200). PECVD oxide was formed by the thermal oxidation of silane at temperatures of 250-350°C and was polished using a lapping tape. The oxide on the PECVD coated pins was about 5 μm thick. Single-crystal silicon pins of orientation (111) ion implanted with C^+ ions at 2-4 mA cm^{-2} current densities, 100 keV accelerating voltage and at a fluence of 1 x 10^{17} ions cm^{-2} were also tested. Silicon pins used for macrotribological studies were also used for microtribological studies.

III. RESULTS AND DISCUSSION

A. Macrotribological studies

Sliders are expensive to produce compared to pins and hence it would be advantageous to conduct tribo-testing with pins. This requires that pin and slider tribological behavior be similar, so that results from tribo-testing with pins can serve as a useful guide in the choice of slider material. The variation of the coefficient of friction with number of sliding cycles for an alumina/titanium-carbide pin and slider

tested under the same load-speed-environment conditions is shown in Fig. 1a. The results suggest that the frictional behavior of pins is reasonably similar to that of sliders.

The objective of this study was to evaluate the potential of using silicon as a slider material. A failure criteria was established which was that a significant increase in friction with number of revolutions was considered a failure since an increase in friction implies some degradation of the interface. In the present investigation it was observed that for single-crystal silicon sliding against lubricated thin-film disks the coefficient of friction was 0.2 at the start of sliding and increased to 0.4 before decreasing to a steady state value of 0.1. Using this as a standard for comparison the number of revolutions before the friction increased by a factor of two was taken to be indicative of the contact life or durability of the slider-disk interface for the various tests conducted. For quick reference, friction data obtained from the various tests conducted in ambient air in terms of the initial coefficient of friction, the contact life, i.e. the number of revolutions before the coefficient of friction increased by a factor of two, the maximum value of the coefficient of friction for cases when the increase was more than by a factor of two are presented in Table 1. For the case of oxidized samples a significant increase (by a factor of two or more) was not observed and so the range of variation of the coefficient of friction for the duration of 50,000 cycles is indicated.

The variation of the coefficient of friction with sliding cycles for single-crystal silicon sliding against lubricated and unlubricated disks in air is shown in Fig. 1b. Crystalline orientation of silicon has no effect on friction and wear. Scanning electron microscopy and chemical analysis using energy dispersive analysis of x-rays (EDAX) suggested that the rise in the coefficient of friction and damage on the pin surface for single-crystal silicon is associated with the transfer of amorphous carbon from the disk to the pin, oxidation-enhanced fracture of pin material followed by tribochemical oxidation of the transfer film. Against lubricated disks the coefficient of friction drops to a steady-state value of 0.1 following the increase as seen in Fig. 1b. This is associated with the formation of a transfer coating on the pin, Fig. 2a. The mechanism of transfer and tribochemical oxidation was seen to be operative for the friction increase for Al_2O_3-TiC and Mn-Zn Ferrite pin/slider materials tested in ambient air. As seen in Table 1 and Fig. 1c, dry oxidized silicon exhibits excellent characteristics in lubricated sliding and this behavior has been attributed to the chemical passivity of the oxide and lack of transfer of DLC carbon

from the disk to the pin. The behavior of PECVD was comparable to that of dry oxide but for the wet oxide there was some variation in the coefficient of friction (0.26-0.4). The difference between dry and wet oxide has been attributed to increased porosity of the wet oxide[5,14].

Since tribochemical oxidation was determined to be a significant factor, experiments were conducted in dry nitrogen. The variation of the coefficient of friction for a silicon pin sliding against a lubricated thin-film disk is shown in Fig. 1d. For comparison the behavior in ambient is also shown. It is seen that in a dry nitrogen environment the coefficient of friction of single-crystal silicon sliding against lubricated disks decreased from an initial value of about 0.2 to 0.05 with continued sliding. Similar behavior was also observed while testing with Al_2O_3-TiC and Mn-Zn Ferrite pins and sliders. With unlubricated disks though the friction decrease was not observed. Based on scanning electron microscopy and chemical analysis this behavior has been attributed to the formation of a smooth amorphous-carbon/lubricant transfer patch and suppression of oxidation in a dry nitrogen environment, Fig. 2b.

The experiments in dry nitrogen indicated that low friction conditions can be achieved in dry nitrogen although transfer of carbon from the disk to the pin occurs. An experiment was performed with a hydrogenated amorphous carbon coated (~ 18 nm thick) silicon pin sliding against a lubricated thin-film disk in dry nitrogen. The friction variation with sliding for this experiment is shown in Fig. 3. No damage for the pin and disk surfaces could be detected after this experiment.

B. Microtribological studies

A summary of micro-scale friction, nanoscratching, nanowear and nanohardness data for various samples is presented in Table 2. Virgin and modified silicon surfaces could be scratched at 10 μN load, see Figs. 4 and 5 and Table 2. Scratch depth increased with an increase in load. We note that crystalline orientation of silicon has little influence on the scratch depth, similar to observations made in macrotribological tests. PECVD-oxide samples had the largest scratch resistance followed by dry-oxidized, wet-oxidized and ion-implanted samples. Ion implantation showed no inprovements on the scratch resistance. By scanning the sample (in 2D) while scratching, wear scars were generated on the sample surface. Wear data on selected samples are presented in Table 2 and the wear profiles at 40 μN of load are shown in Fig. 6. PECVD-oxide samples had the largest wear resistance followed by dry-

oxidized, wet-oxidized and ion-implanted samples. These results are consistent with the macrotribological data. We observed wear debris in the wear zone just after the wear test which could be easily removed by scanning the worn region. It suggests that wear debris is loose.

We further studied the wear resistance of ion-implanted samples, Fig. 7. For tests conducted at various loads on Si (111) and C^+-implanted Si (111), we find that wear resistance of implanted sample is slightly poorer than that of virgin Si up to about 80 μN. Above 80 μN, the wear resistance of implanted Si improves. As we continue to run tests at 40 μN for larger number of cycles, implanted sample exhibits higher wear resistance than unimplanted sample. Miyamoto et al.[15] have also reported that damage from the implantation in top layer results in poorer wear resistance, however, implanted zone at the subsurface is more wear resistant than the virgin Si.

We measured nanoindentation hardness of all samples, Table 2. Coatings and treatments improved nanohardness of silicon. We note that dry-oxidized and PECVD films are harder than wet oxidized films as these films may be porous[5]. High hardness of oxidized films may be responsible for measured low wear on macro and micro scale. Figure 8 shows the indentaion marks generated on virgin and C^+-implanted Si (111) at 70 μN. The depth of indentation was about 3 nm. Hardness values of virgin and C^+-implanted Si (111) at various indentation depths (normal loads) are presented in Fig. 9. The calculated hardness value for virgin Si at an indentation depth of about 7 nm (normal load of 100 μN) is about 11.7 GPa, comparable to nanohardness values reported by others[16]. We note that the surface layer of the implanted zone is much harder compared to the subsurface, and may be brittle leading to higher wear on the surface. Subsurface of the implanted zone is harder than the virgin silicon, resulting in higher wear resistance.

From the data presented in Tables 1 and 2, we note that macro-and micro-coefficient of friction values of all samples are about the same with the microvalues lower than the macro values. Roughness effects on the friction of polysilicon can be clearly observed. Next we examine the relationships between friction and roughness profiles, Fig. 10. We find that there is no resemblance between the coefficient of friction profiles and the corresponding roughness profiles, e.g., high or low points on the friction profile do not correspond to high or low points on the roughness profiles. We calculated the slope of the roughness profile in the tip sliding direction. By comparing the resulting slope profile and

corresponding friction profiles, we observe a strong correlation between the two. Surface slope and friction profiles obtained with sample sliding in either direction are shown in Fig. 11. We again note the resemblance between local variations in the surface slope and local variations in friction. We further note the directionality in friction. Bhushan and Ruan[12] have shown that the local variation in friction arises from a "ratchet" mechanism. According to this mechanism, friction increases as the FFM tip slides over the leading (ascending) edge of asperity because of a positive surface slope. Friction decreases during sliding over the trailing (descending) edge of the asperity as the slope is negative. The ratchet mechanism thus explains the correlation between the slopes of the roughness profiles and friction profiles observed in Fig. 10. Since the local friction is a function of the local slope of sample surface, the local variation in friction should be of the opposite sign as the scanning direction is reversed. In Fig. 11(c), the sign of friction in one direction is reversed, but we still see some difference in the two friction profiles which may result from the asymmetrical asperities.

IV. CONCLUSIONS

Our investigation suggests that transfer and tribochemical oxidation are significant factors affecting the friction and wear performance of the head-disk interface. Nanoscratch/nanowear and nanoindentation studies suggest that coated silicon is superior to that of virgin silicon, similar to that found in macrotribological tests . It appears that with appropriate coatings to combat transfer and tribochemical oxidation, such as dry oxide or PECVD SiO_2 in ambient air and amorphous carbon in dry nitrogen environments, silicon is an excellent candidate material for the construction of magnetic head sliders. In this paper, we have reported an example of indentation hardness measurements at a penetration depth of about 3 nm, which is lower than that can be achieved with an indenter available to date.

This research was sponsored in part by the Office of the Chief of Naval Research (Department of Navy), Advanced Research Projects Agency/National Storage Industry Consortium; and the Membership of the CMCL.

References

[1]K.E. Petersen, *Proc. IEEE,* **70**, No. 5, 420-457 (1982).

[2]B. Bhushan and S. Venkatesan, *Adv. Info. Storage Syst.*, **5**, 211-239 (1993).

[3]J. P. Lazzari and P. Deroux-Dauphin, *IEEE Trans. Mag.*, **25**, No. 5, 3190-3193 (1989).

[4]B. Bhushan, M. Dominiak, and J.P. Lazzari, *IEEE Trans. Magn.*, **28**, 2874-2876 (1992).

[5]B. Bhushan and S. Venkatesan, *J. Mater. Res,* **8**, 1611-1628 (1993).

[6]S. Venkatesan and B. Bhushan, *Adv. Info. Storage Syst.*, **5**, 243-257 (1993).

[7]S. Venkatesan and B. Bhushan, *Wear* (1993) (in press).

[8]B.K. Gupta, J. Chevallier, and B. Bhushan, *J. Trib.*, Trans. ASME, **115**, 392-399 (1993).

[9]B.K. Gupta, J. Chevallier, and B. Bhushan, *Trib. Trans.* (1993) (in press).

[10]B. Bhushan, *Tribology and Mechanics of Magnetic Storage Devices* (Springer Verlag, New York, 1990).

[11]J. Ruan and B. Bhushan, *J. Trib.*, Trans. ASME (in press).

[12]B. Bhushan and J. Ruan, *J. Trib.*, Trans. ASME (in press).

[13]B. Bhushan, V.N. Koinkar, and J. Ruan, *J. Eng. Trib.*, Proc. I. Mech. E. (in press).

[14]W. A. Pilskin, *J. Vac. Sci. Tech. nol.,* **14**, 1064-1081 (1977).

[15]T. Miyamoto, S. Miyake, and R. Kaneko, *Proc. 1st Int. Workshop on Microtribology*, Jap. Soc. Tribologists, 258-265 (1993).

[16]G.M. Pharr, W.C. Oliver, and D.R. Clarke, *J. Electronic Mat.*, **19**, No. 9, 881-887 (1990).

Table 1 Macro friction data for various pin materials sliding against thin-film rigid disks in ambient air. Normal load = 0.5 N; sliding speed = 0.9 - 1.2 m/s; ambient air (R.H. 45±5%).

Pin Material	Initial coeff. of friction	Cycles to friction increase by factor of two	Max. or ending value of Coeff. of friction
Al_2O_3-TiC	0.20 - lubed 0.25 - unlubed	~2200 - lubed ~200- unlubed	0.78 - lubed 0.78 - unlubed
Mn-Zn Ferrite	0.22 - lubed 0.22 - unlubed	~5500 - lubed ~600 - unlubed	0.45 - lubed 0.68 - unlubed
Single- crystal silicon	0.20 - lubed 0.20 - unlubed	~1200 - lubed ~500 - unlubed	0.40 - lubed 0.70 - unlubed
Polysilicon	0.20 - lubed 0.22 - unlubed	~3000 - lubed ~1000 -unlubed	0.60 - lubed 0.50 - unlubed
PECVD-oxide coated Si (111)	0.28 - lubed 0.28 - unlubed	>50,000 -lubed ~500 - unlubed	0.23-0.28 (lub) 0.72 - unlubed
Dry-oxidized Si (111)	0.22 - lubed 0.22 - unlubed	>50,000 -lubed ~1000- unlubed	0.20 - lubed 0.56 - unlubed
Wet-oxidized Si (111)	0.26 - lubed 0.26 - unlubed	>50,000-lubed ~1000- unlubed	0.26-0.40 (lub) 0.60 - unlubed
C^+-implanted Si (111)	0.16 - lubed 0.25- unlubed	~1000 - lubed ~1000 -unlubed	0.60 - lubed 0.50 - unlubed

Table 2. Microfriction, nanoscratching/nanowear, and nanoindentation hardness data for various virgin coated and treated silicon samples.

Material	Rms roughness, scan size: 500 nm x 500 nm (nm)	Coeff. of friction	Scratch depth at 40μN (nm)	Wear depth at 40μN (nm)	Hardness at 5 μN (GPa)
Si (111)	0.11	0.03	20	27	11.7
Si (110)	0.09	0.04	20		
Si (100)	0.12	0.03	25		
Polysilicon	1.07	0.04	18		
Polysilicon (lapped)	0.16	0.05	18	25	12.5
PECVD oxide - coated Si (111)	1.50	0.01	8	5	18.0
Dry-oxidized Si (111)	0.11	0.04	16	14	17.0
Wet-oxidized Si (111)	0.25	0.04	17	18	14.4
C^+-implanted Si (111)	0.33	0.02	20	23	18.6

Figure Captions

Fig. 1. Variation of the coefficient of friction with number of sliding cycles in ambient air (a) Al_2O_3-TiC pin and slider against a lubricated disk, (b) Si (111) pin against a lubricated and unlubricated disk, (c) dry oxidized Si pin against a lubricated disk, (d) Si (111) against a lubricated disk in ambient air and dry nitrogen.

Fig 2. SEM micrographs of Si (111) after sliding against a lubricated disk in (a) ambient air for 6000 cycles, and (b) in dry nitrogen after 15,000 cycles.

Fig. 3. Variation of the coefficient of friction with number of sliding cycles in dry nitrogen for a DLC coated silicon pin sliding against a lubricated disk.

Fig. 4. Scratch depth as a function of load after ten cycles for virgin, treated, and coated Si surfaces.

Fig. 5. Surface profiles for scratched (a) Si (111), (b) PECVD-oxide coated Si (111), (c) dry-oxidized Si (111), and (d) C^+-implanted Si (111). The loads used for various scratches at ten cycles are indicated in the plot.

Fig. 6. Surface profiles showing the worn region (center 2 μm x 2 μm) after one cycle of wear at 40 μN load (a) Si (111), (b) PECVD-oxide coated Si (111), (c) dry-oxidized Si (111), and (d) C^+-implanted Si (111).

Fig. 7. Wear depth as a function of (a) load (after one cycle), and (b) cycles (normal load = 40 μN) for Si (111) and C^+-implanted Si (111).

Fig. 8. Gray scale plot and line plot of the inverted nanoindentation mark on (a) Si (111) at 70 μN (hardness ~15.8 GPa), and (b) gray scale plot of indentation mark on C^+-implanted Si (111) at 70 μN (hardness ~16.2 GPa). The indentation depth of indent was about 3 nm.

Fig. 9. Nanohardness and normal load as function of indentation depth for virgin and C^+-implanted Si (111).

Fig. 10. Surface roughness profile (σ= 1.07 nm), (b) slope of the roughness profile along the sample sliding direction (the horizontal axis) (mean = -0.02, σ = 0.05), and friction profile (mean = 5.8 nN, σ = 1.3 nN) of rough polysilicon for a normal load of 140 nN.

Fig. 11. Gray-scale plots of (a) the slope of the surface roughness, (b) the friction, and (c) the friction (with sign reversed in the right hand profile) of a Si (111). The left side of the figure corresponds the sample sliding from left to right. Higher points are shown by lighter color.

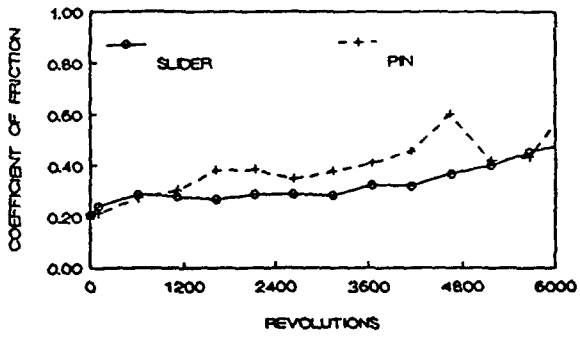
1.00
0.80
0.60
0.40
0.20
0.00
COEFFICIENT OF FRICTION
SLIDER
PIN
0
1200
2400
3600
4800
6000
REVOLUTIONS

(a)

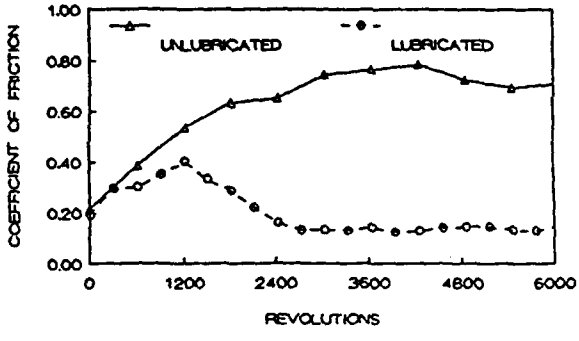
1.00
0.80
0.60
0.40
0.20
0.00
COEFFICIENT OF FRICTION
UNLUBRICATED
LUBRICATED
0
1200
2400
3600
4800
6000
REVOLUTIONS

(b)

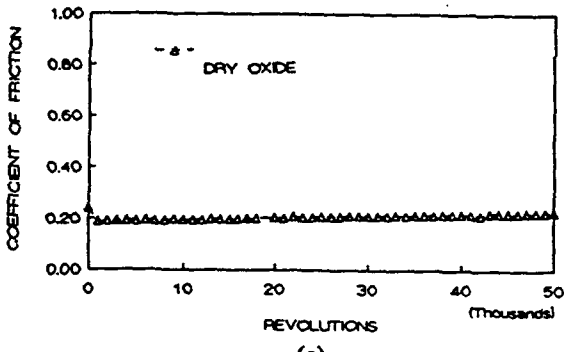
1.00
0.80
0.60
0.40
0.20
0.00
COEFFICIENT OF FRICTION
DRY OXIDE
0
10
20
30
40
50
(Thousands)
REVOLUTIONS

(c)

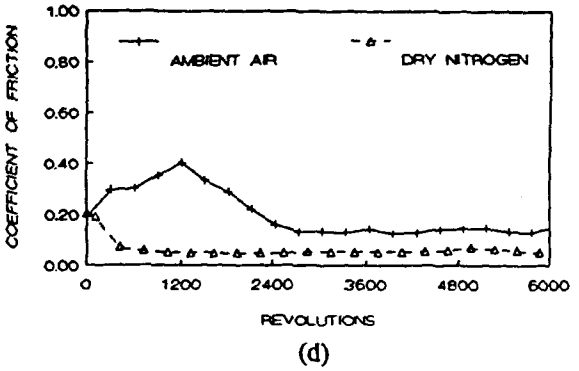
1.00
0.80
0.60
0.40
0.20
0.00
COEFFICIENT OF FRICTION
AMBIENT AIR
DRY NITROGEN
0
1200
2400
3600
4800
6000
REVOLUTIONS

(d)

Fig. 1

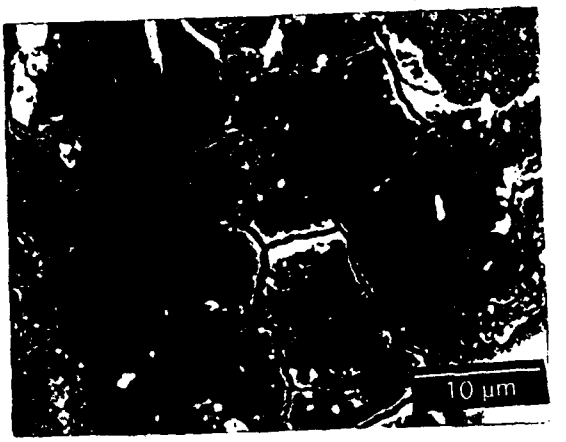

(a)

(b)

Fig. 2

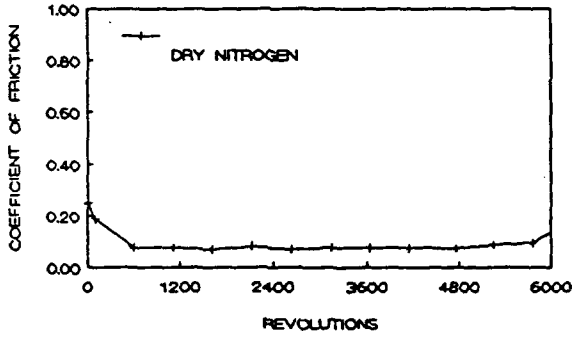
1.00
0.80
0.60
0.40
0.20
0.00
COEFFICIENT OF FRICTION
DRY NITROGEN
0
1200
2400
3600
4800
6000
REVOLUTIONS

Fig. 3

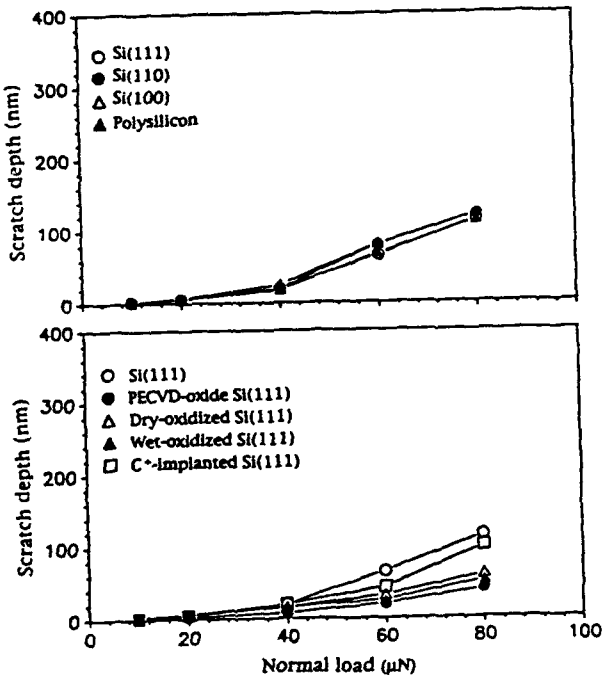
Scratch depth (nm)
400
300
200
100
0
Si(111)
Si(110)
Si(100)
Polysilicon
Scratch depth (nm)
400
300
200
100
0
Si(111)
PECVD-oxide Si(111)
Dry-oxidized Si(111)
Wet-oxidized Si(111)
C+-implanted Si(111)
0
20
40
60
80
100
Normal load (μN)

Fig. 4

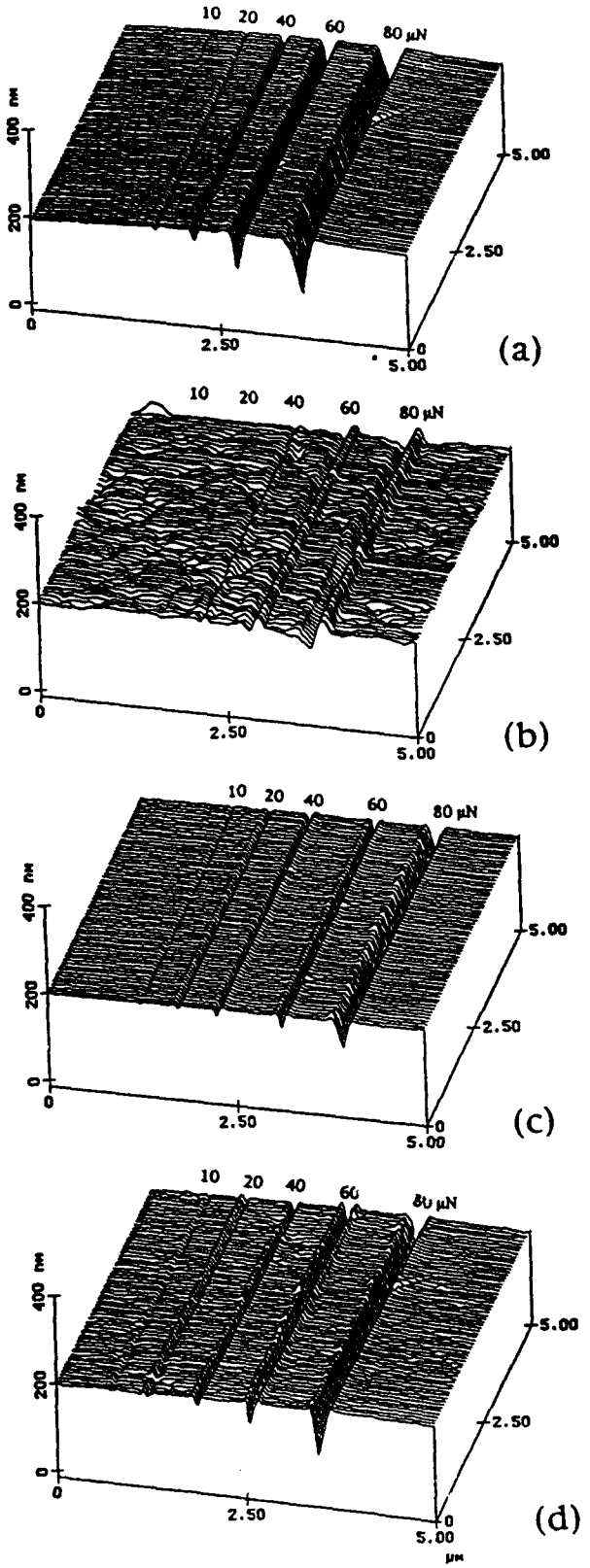

Fig. 5

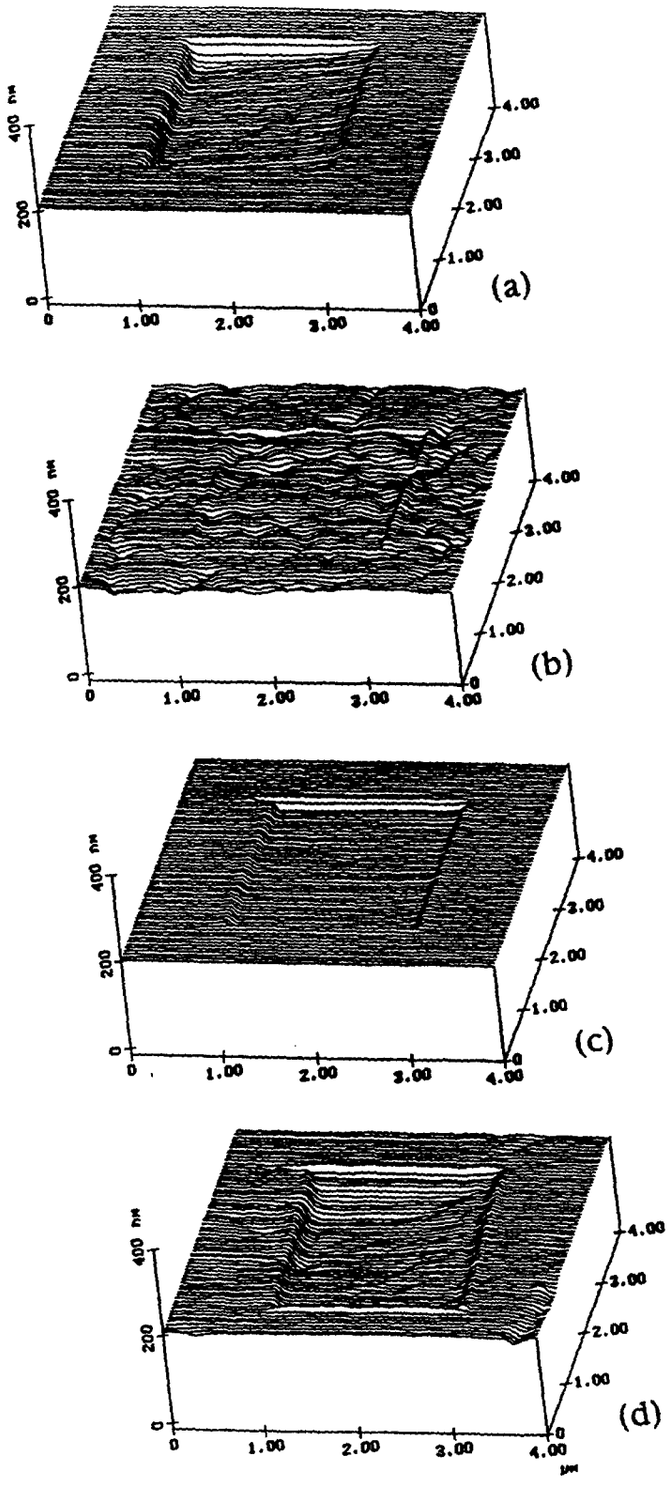

Fig. 6

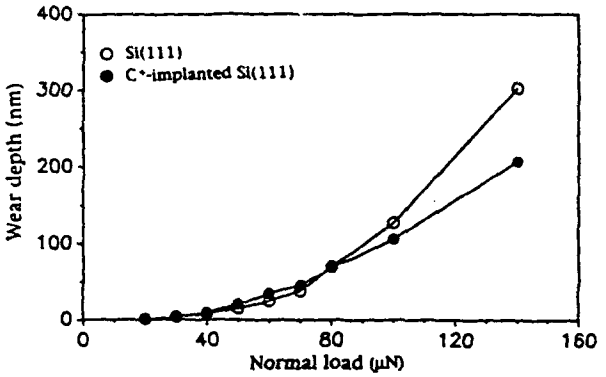
400
300
200
100
0
Wear depth (nm)
Si(111)
C+-implanted Si(111)
0
40
80
120
160
Normal load (μN)

(a)

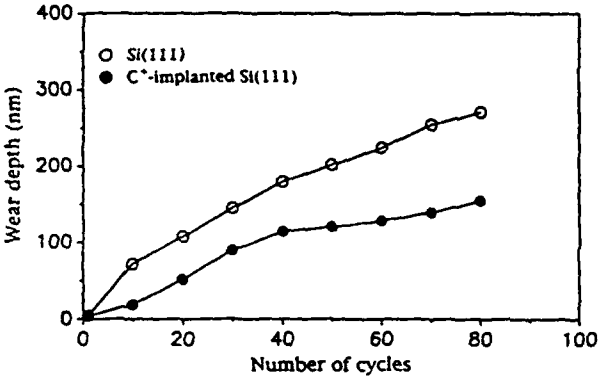
400
300
200
100
0
Wear depth (nm)
Si(111)
C+-implanted Si(111)
0
20
40
60
80
100
Number of cycles

(b)

Fig. 7

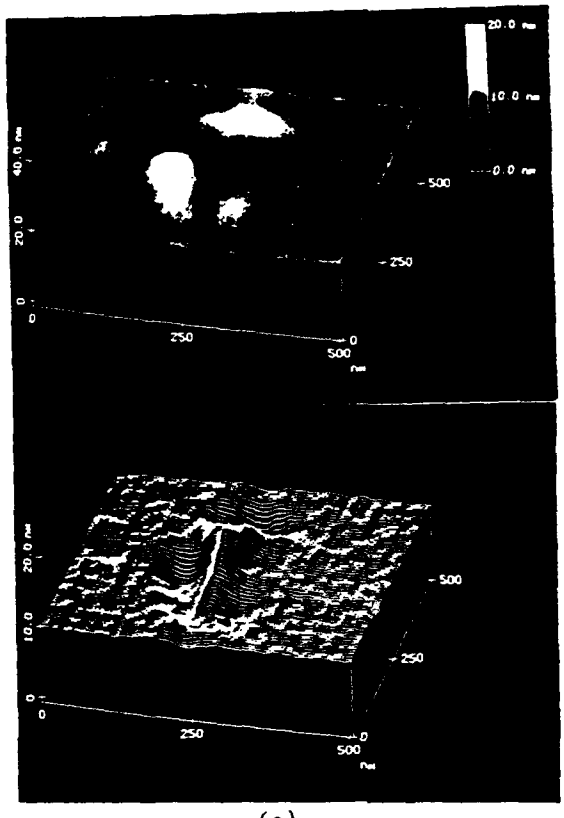
20.0 nm
10.0 nm
0.0 nm
40.0 nm
20.0
0
0
250
500
nm
20.0 nm
10.0
500
250

(a)

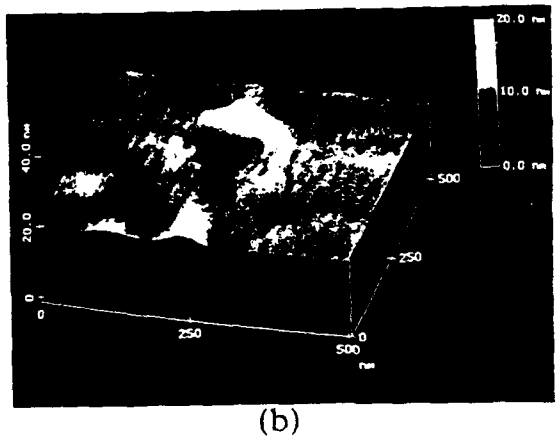
20.0 nm
10.0 nm
0.0 nm
40.0 nm
20.0
0
0
250
500
nm

(b)

Fig. 8

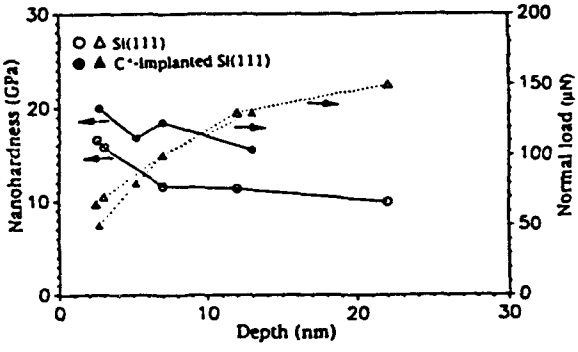
Nanohardness (GPa)
Normal load (μN)
Depth (nm)
Si(111)
C+-implanted Si(111)
0
10
20
30
50
100
150
200

Fig. 9

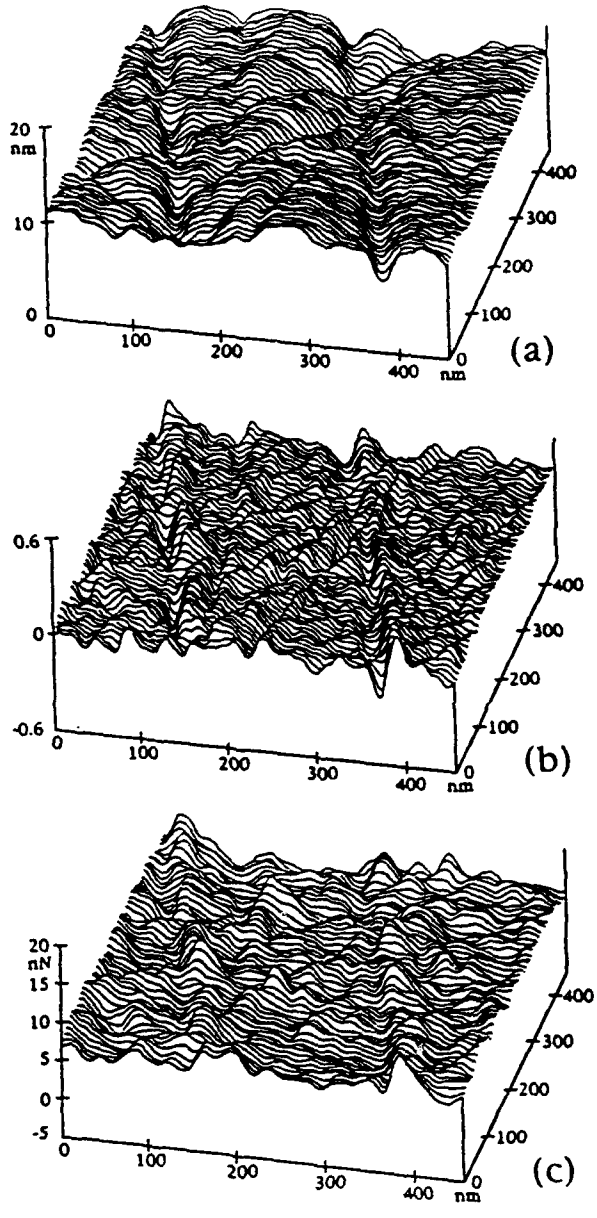
20
nm
10
0
0
100
200
300
400
nm
400
300
200
100
0
(a)
0.6
0
-0.6
0
100
200
300
400
nm
400
300
200
100
0
(b)
20
nN
15
10
5
0
-5
0
100
200
300
400
nm
400
300
200
100
0
(c)

Fig. 10

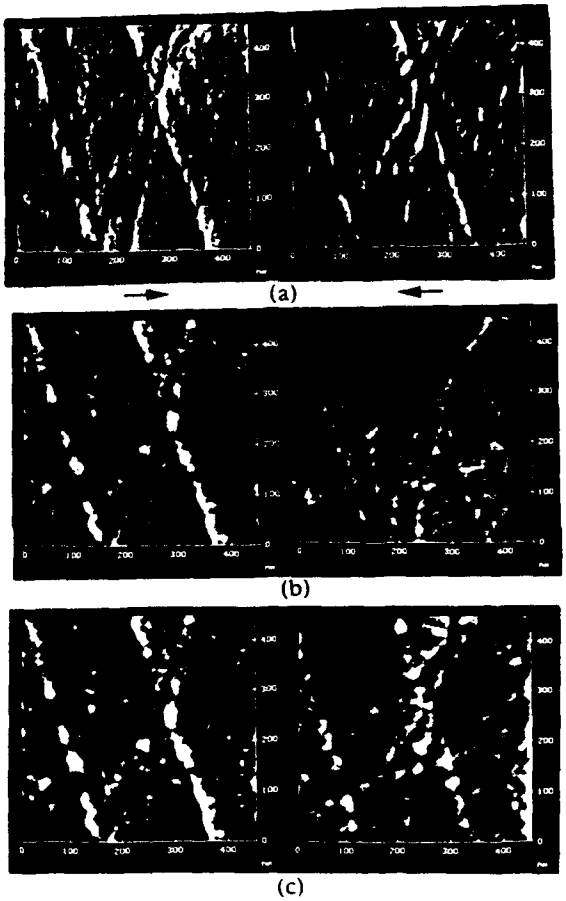

Fig. 11